Clinical Oral Implants Research

WILEY

CLINICAL ORAL IMPLANTS RESEARCH

ORIGINAL ARTICLE OPEN ACCESS

Antibacterial Effect of Combined Electrolytic and Chemical Decontamination Methods on Dental Implant Surfaces: In Vitro Study

Verónica Odeh[1] | Leire Virto[1,2] | Enrique Garcia-Quismondo[3] | David Herrera[1] | Jesús Palma[3] | Mariano Sanz[1]

[1]Etiology and Therapy of Periodontal and Peri-Implant Diseases (ETEP), research Group, University Complutense, Madrid, Spain | [2]Department of Anatomy and Embryology, Faculty of Optics and Optometry, University Complutense of Madrid, Madrid, Spain | [3]Electrochemical Processes Unit, IMDEA Energy, Madrid, Spain

Correspondence: Leire Virto (lvirto@ucm.es)

Received: 27 February 2025 | **Revised:** 21 July 2025 | **Accepted:** 22 July 2025

Funding: This study was partially funded by a research contract between the ITI Foundation and the University Complutense of Madrid (Project No. 1320-2018).

Keywords: antiseptics | biofilm | chlorhexidine | dental implant | electrochemical | peri-implantitis

ABSTRACT

Objectives: To evaluate the combined effect of direct electrical current and chlorhexidine digluconate (CHX) for decontaminating titanium implant surfaces, using a validated in vitro oral multispecies biofilm model.

Material and Methods: Contaminated implant surfaces were tested using an electrochemical cell consisting of a three-electrode system immersed in a KI-AL electrolyte, the biofilm-coated implant being the working electrode, a platinum mesh the counter electrode, and an Ag/AgCl electrode the reference. Direct electrical currents (DC) were applied at two voltage levels (-3 V and −0.75 V) for 5 min, followed by a 1-min rinse in 0.12% CHX. The results were compared to 0.12% CHX alone. Untreated contaminated implants served as negative controls. The antibiofilm effect was evaluated by quantitative polymerase chain reaction with propidium monoazide and by scanning electron microscopy in three different implant zones (threads, valleys and transmucosal machined neck). The area of residual bacteria was also calculated by image analysis.

Results: The combined treatment significantly reduced the viable total bacterial counts ([-3 V + CHX] = 4.6 and [−0.75 V + CHX] = 4.9 logarithm colony forming units-LogCFU/mL), compared to the negative control group (6.1 LogCFU/mL) and 0.12% CHX alone (6.3 LogCFU/mL). The area of residual bacteria was also significantly reduced, removing over 95% of the biofilm in combined treatment groups, with slightly higher efficiency at -3 V. Electrolytic cleaning was able to reach all implant zones and no significant differences were found between [-3 V + CHX] and [−0.75 V + CHX] for any parameter.

Conclusion: The proposed combined treatments were more effective in reducing the vitality of multispecies biofilms on implant surfaces compared to CHX alone.

1 | Introduction

Peri-implantitis represents a chronic inflammatory condition characterized by progressive bone loss and subsequent exposure of the implant surface (Schwarz et al. 2018). The management of the exposed and contaminated implant surface remains one of the challenges in the management of this disease. To date, a great variety of mechanical and chemical strategies have been evaluated both in vitro and in clinical studies, but none has demonstrated a significant superiority in reducing or eliminating the biofilms adhered to the implant surfaces, without exerting at the same time a detrimental effect on the implant surface. This inability to properly decontaminate affected implant surfaces may be one of the key factors

why the long-term results of the treatment of peri-implantitis are unpredictable and have high rates of disease recurrence (Cosgarea et al. 2023; de Waal et al. 2023; Ramanauskaite et al. 2023; Wilensky et al. 2023).

In recent years, a strategy based on electrical stimulation of the affected implant surfaces has emerged as a potential tool for peri-implant biofilm control (Al-Hashedi et al. 2016; Virto et al. 2023; Del Pozo et al. 2008; Ehrensberger et al. 2015; Koch et al. 2020; Mohn et al. 2011; Sahrmann et al. 2014; Schneider et al. 2018; Sultana et al. 2015). These investigations have led to the availability of a medical device to treat peri-implantitis based on electrochemical decontamination of implant surfaces (GalvoSurge Dental Implant Cleaning System, GalvoSurge Dental AG, Widnau, Switzerland). Results from the use of this device in clinical studies have resulted in the improvement of clinical parameters and radiographic bone fill after regenerative therapy (Schlee et al. 2021), although these studies do not demonstrate the efficacy to treat peri-implantitis, given the lack of a control group. In addition, this device uses high-intensity electrical currents, which may cause not only biofilm removal but also tissue damage. In fact, manufacturers only recommend its surgical use once the tissues have been reflected and with intense local anesthesia of the region of treatment.

In contrast, our research group has recently published (Virto et al. 2023) the ability of an innovative electrochemical treatment using low-intensity electrical currents (a constant-voltage pulse of −3 V during a short exposure of 5 min) to affect the structure and vitality of a 72-h mature multispecies oral biofilm, being able to reduce the total bacterial load in >99%, while low potential had no antibacterial effects. Some authors have suggested that low-intensity electrical currents do not have a bactericidal effect, but are capable of improving the antibiofilm efficacy of antimicrobials, what is termed the "bioelectric effect" (Blenkinsopp et al. 1992; Freebairn et al. 2013; Lasserre et al. 2015; Nodzo et al. 2015). This effect has been demonstrated by significantly enhancing the efficacy of different antibiotics (Blenkinsopp et al. 1992; Canty et al. 2017; Ehrensberger et al. 2015; Jass et al. 1995; Jass and Lappin-Scott 1996; Lasserre et al. 2015; Nodzo et al. 2015; Stewart et al. 1999; Sultana et al. 2015; Suttasattakrit et al. 2021; Zou et al. 2022). However, this effect has not been tested by combining electric currents and broadly used oral antiseptics. It was, therefore, the objective of this in vitro investigation to evaluate the antibiofilm effect of combining direct electrical currents with chlorhexidine digluconate on contaminated implant surfaces, using a validated oral multispecies biofilm model.

2 | Material and Methods

2.1 | In Vitro Multi-Species Biofilm Model

Ethical approval was not required for this in vitro study. In brief, the selected in vitro biofilm model (Sanchez et al. 2014) includes six oral bacteria (*Streptococcus oralis* CECT 907 T, *Veillonella parvula* NCTC 11810, *Actinomyces naeslundii* ATCC 19039, *Fusobacterium nucleatum* DMSZ 20482, *Aggregatibacter actinomycetemcomitans* DSMZ 8324 and *Porphyromonas gingivalis* ATCC 33277), first grown on blood agar plates (Blood Agar Oxoid N° 2; Oxoid, Basingstoke, UK), supplemented with 5% (v/v) sterile horse blood (Oxoid), 5.0 mg L^{-1} hemin (Sigma, St. Louis, MO, USA) and 1.0 mg L^{-1} menadione (Merck, Darmstadt, Germany) in anaerobic conditions (10% H_2, 10% CO_2, and balance N_2) at 37°C ± 1°C for 24–72 h. Then, pure cultures of each bacterium were grown anaerobically in a protein-rich medium containing brain-heart infusion (BHI) (Becton, Dickinson and Company, Franklin Lakes, NJ, USA) supplemented with 2.5 g L^{-1} mucin (Oxoid), 1.0 g L^{-1} yeast extract (Oxoid), 0.1 g L^{-1} cysteine (Sigma-Aldrich), 2.0 g L^{-1} sodium bicarbonate (Merck, NJ, USA), 5.0 mg L^{-1} hemin (Sigma-Aldrich) and 1.0 mg L^{-1} menadione (Merck) and 0.25% (v/v) glutamic acid (Sigma-Aldrich). Once the bacterial concentration was adjusted by spectrophotometry, solutions of 10^3 colony forming units (CFU)/mL for *S. oralis*, 10^5 CFU/mL for *V. parvula* and *A. naeslundii*, and 10^6 CFU/mL for *F. nucleatum*, *A. actinomycetemcomitans*, and *P. gingivalis* were pooled in the BHI medium and added over sterile titanium implants, 3.3 mm in diameter and 8 mm height (Roxolid SLA implant, Straumann, Basel, Switzerland) and incubated in anaerobic conditions (10% H_2, 10% CO_2 and balance N_2) at 37°C ± 1°C for up to 72 h of incubation (Bermejo et al. 2019). As negative controls, implant surfaces were bathed with culture medium without bacteria.

2.2 | Electrolytic Model

The electrolytic cell used for the electrochemical decontamination of implants has been described in detail in the previous publication from our research group (Virto et al. 2023). In brief, it consists of a three-electrode electrochemical cell where the direct currents (DC) are applied using constant potential, the contaminated titanium implant (Straumann, S ø3.3 mm RN SLA Roxolid, Loxim) being the working electrode (WE); a platinum mesh (Custom-built, ø 1.2 cm), the counter electrode (CE); and an Ag/AgCl, the reference electrode (RE) (Figure 1). The electrolyte was a solution of potassium iodide and L lactic acid (KI-LA) (1 M pH = 6.4) (Schneider et al. 2018). The electrical polarization was applied using a dedicated potentiostat (VersaSTAT 3–200; Princeton Applied Research, USA).

2.3 | Implant Surface Decontamination Methods

The tested implant surface decontamination protocols consisted of four groups:

- Two groups combining the electrolytic effect of very low (−0.75 V) or low (−3 V) constant-voltage pulses (DC) with the chemical effect of 0.12% chlorhexidine digluconate (CHX) (Merck, Darmstadt, Germany): [−3 V + CHX] and [−0.75 V + CHX]. Implants were first subjected to electrical current during 5 min and then were immersed and rinsed with 0.12% CHX in cell-culture plates during 1 min (Solderer et al. 2019).
- A group applying 0.12% CHX alone to the implant surfaces during 1 min [CHX].
- A group applying the electrolytic KI-AL solution during 5 min [E].

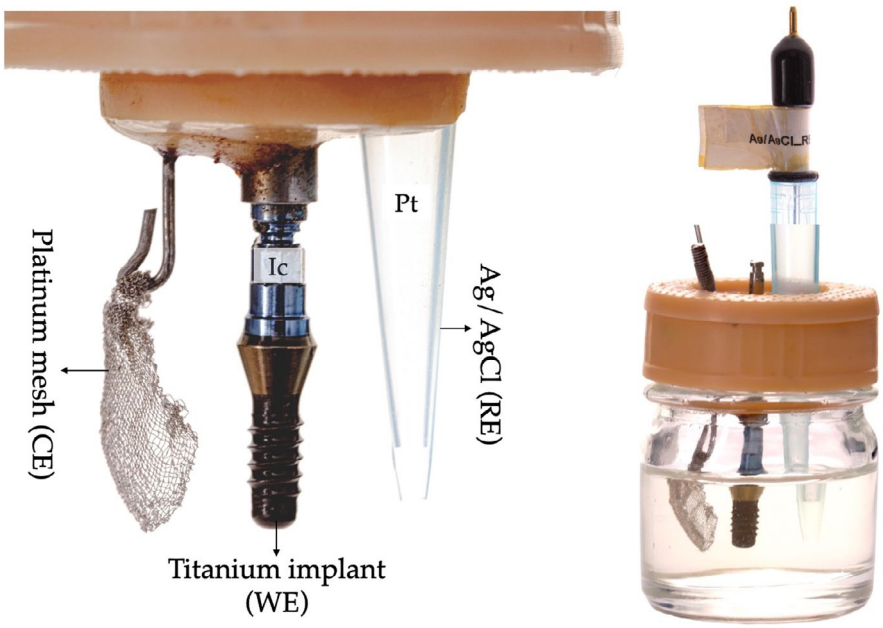

FIGURE 1 | Custom-designed, three-electrode potentiostatic, electrochemical stimulation chamber. The working electrode is the titanium implant on which a 72-h biofilm has been incubated, located between the Ag/AgCl electrode (reference) and the platinum electrode (counter). CE, Counter-electrode; WE, Working Electrode; RE, Reference electrode; Ic, Implant carrier; Pt, Pipette tip.

In addition, a negative control group with untreated biofilm-contaminated implant surfaces [C] was included. Each protocol was performed in triplicate.

3 | Outcomes Measurements

3.1 | Quantification of Live Bacteria

The experimental design included three independent experiments, each with three replicas ($n = 9$). After applying the surface decontamination methods, implants were removed from the electrolytic cell and rinsed three times in 10 mL of sterile phosphate buffer saline (PBS) for 10 s per rinse each to eliminate nonadherent bacteria. After that, biofilm was disrupted by vortexing for 3 min and treated with propidium monoazide (PMA) (Biotium Inc., Hayword, CA, USA) to discriminate DNA from live versus dead bacteria (Sánchez et al. 2014). Then, DNA was isolated from the resulting pellet using a commercial kit (MoIYsis Complete5. Molzym Gmbh & Co.KG. Bremen, Germany), following the manufacturer's instructions. The hydrolysis probe 5′ nuclease assay, quantitative polymerase chain reaction (qPCR) method, was used for detecting and quantifying the bacterial DNA from live cells. Primers and probes were obtained from Life Technologies Invitrogen (Carlsbad, CA, USA), Applied Biosystems (Carlsbad, CA, USA) and Roche (Roche Diagnostic GmbH; Mannheim, Germany) and were targeted against 16 S rRNA genes. The sequence and concentration of the primers, as well as the methodology used, have been described in previous studies (Marin et al. 2017; Marin et al. 2018). Each DNA sample was analyzed in duplicate. Quantification cycle (Cq) was determined using the provided software package (LC480 Software1.5; Roche). Quantification of cells by qPCR was based on standard curves. The correlation between Cq values and CFU/mL was automatically generated through the software (LC480Software1.5; Roche).

3.2 | Scanning Electron Microscope (SEM) and Image Analysis

The biofilm structure was also studied by scanning electron microscopy JSM 6400 (JSM6400; JEOL, Tokyo, Japan). The experimental design included three independent experiments, each with two replicas ($n = 6$). After applying the surface decontamination methods, first, the implants ($n = 6$) were fixed in a solution of 4% paraformaldehyde and 2.5% glutaraldehyde for 4 h at 4°C. After that, they were washed once in PBS and sterile water (immersion time per washed 10 min) and then dehydrated through a series of graded ethanol solutions (30, 50, 70, 80, 90 and 100%; immersion time per series 10 min). Finally, specimens were critical-point dried, sputter-coated with gold, and analyzed by electron microscopy with a back-scattered electron detector and an image resolution of 25 kV. The implant surface was divided into three regions of interest (ROIs), being the first two moderately rough implant surfaces and the third machined surface: (1) the thread, (2) the valley between two threads, and (3) the transmucosal neck. Images were taken at x2000 and x5000 magnifications.

The area of residual bacteria was further evaluated by image analysis, as previously described by (Ichioka et al. 2023; Vyas et al. 2016). This method uses images taken at x5000 magnification that are converted into 8-bit images and evaluated with Fiji Image analysis software (ImageJ software, US National Institutes of Health, Bethesda, Maryland, USA). Briefly, a global scale is set using a known distance from a SEM image (10 μm). The plugin Trainable Weka Segmentation is then run to produce pixel-based segmentations employing the line selection tool (of 10-pixel width) for the ROIs to add traces into one of two classes, either the implant

surface (class 1) or the biofilm (class 2). At least 10 ROIs were selected for each class to train the algorithm and ensure proper segmentation. It created and displayed a resulting binary image in which the threshold levels were adjusted (low and upper threshold levels were set at 1) so the surface turned into black and the biofilm areas into white. Finally, the area of residual bacteria (biofilm) was selected and measured. The percentage of biofilm remaining was also calculated as follows:

$$\%\,Biofilm\ remaining = \frac{biofilm\ area\ after\ treatment}{biofilm\ area\ in\ untreated\ implants\ (C)} \times 100$$

4 | Statistical Analysis

An experiment-level analysis was performed for each study parameter ($n = 9$). Shapiro–Wilk goodness-of-fit tests and distribution of data were used to assess normality. Data are expressed as means and standard deviations (SD) and 95% confidence intervals (CI). To evaluate the effect of decontamination protocols on bacterial counts (live CFU/mL) and the area of residual bacteria (μm^2) analysis of variance and post hoc testing with Bonferroni's correction were used. Intergroup and intragroup comparisons were made to evaluate differences among groups and implant zones (thread, valley and machined neck). A software package (IBM SPSS Statistics 29.0; IBM Corporation, Armonk, NY, USA) was used for all data analyses. Results were considered statistically significant at $p < 0.05$.

5 | Results

5.1 | Electrochemical Parameters

During polarization, the potentiostat recorded the voltage–time and generated power–time curves (Figure 2). After applying −3 V, the power response depicted two distinct phases. During the first 50 s, the power remained around 20 mW and then increased sharply to 180 mW, ultimately resulting in a total energy consumption of 13.5 ± 20 mWh and an electrical charge of 4.5 ± 7 mAh after 5 min of exposure. However, when applying low voltage, the profile showed a rapid current increase, followed by an exponential decrease approaching zero. This resulted in a more controlled and uniform response, with minimal energy consumption and electrical charge: 0.002 ± 0.001 mWh and 0.002 ± 0.001 mAh, respectively. Therefore, compared to high-voltage conditions, the low-voltage pulse showed significantly lower energy and charge delivery (~99.9% reduction). Details of the power profiles are shown in Figure 2.

5.2 | Effect on Biofilm Vitality

Figure 3 depicts the number of viable bacteria, analyzed by qPCR, remaining after being exposed to the different experimental conditions. Statistically significant reductions in total bacteria were observed in all groups, compared to the control group, being more evident in the combined treatment groups [−3 V + CHX] and [−0.75 V + CHX]. Furthermore, both [−3 V + CHX] and [−0.75 V + CHX] significantly reduced total bacterial counts when compared to [CHX] ($p < 0.001$). Particularly, both test groups were able to significantly reduce all six species of the biofilm, except *A. actinomycetemcomitans*. On the contrary, the [CHX] group was only effective against two species, *A. naeslundii* and *P. gingivalis*. No statistically significant differences were found between lower [−0.75 V + CHX] and higher [−3 V + CHX] potentials (Supplemental Table S1).

When calculating the net effect of the tested treatments as: [(total number of bacteria in biofilms treated with the negative

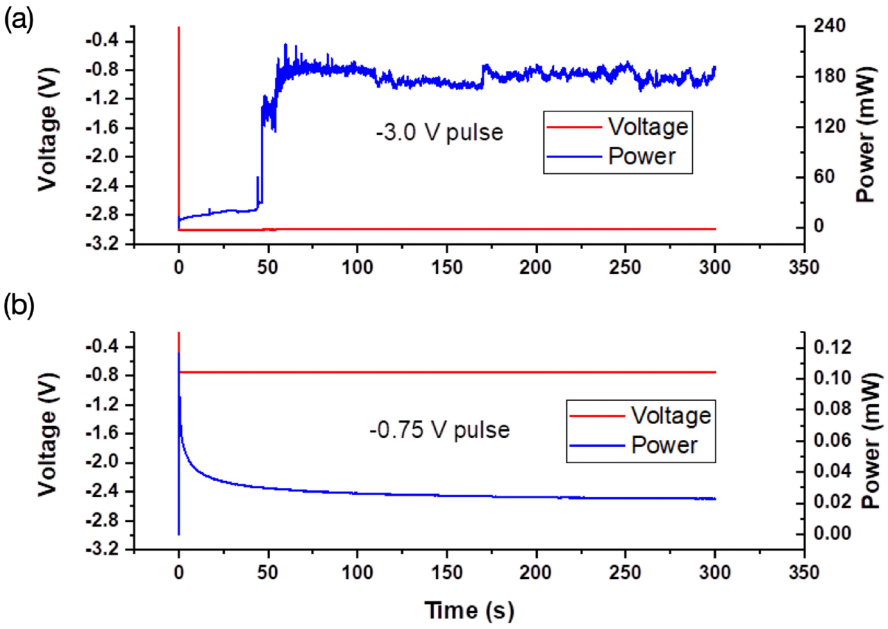

FIGURE 2 | Voltage and power-time curves recorded during potentiostatic stimulation. Panel (a) shows the response for −3 V, which displays an initial low power phase followed by a sharp increase. Panel (b) corresponds to −0.75 V, characterized by a rapid peak and exponential decay of current and power. Voltage is expressed versus the reference electrode (Ag/AgCl), and power is shown in milliwatts (mW). These curves illustrate the significantly lower energy input of the −0.75 V condition.

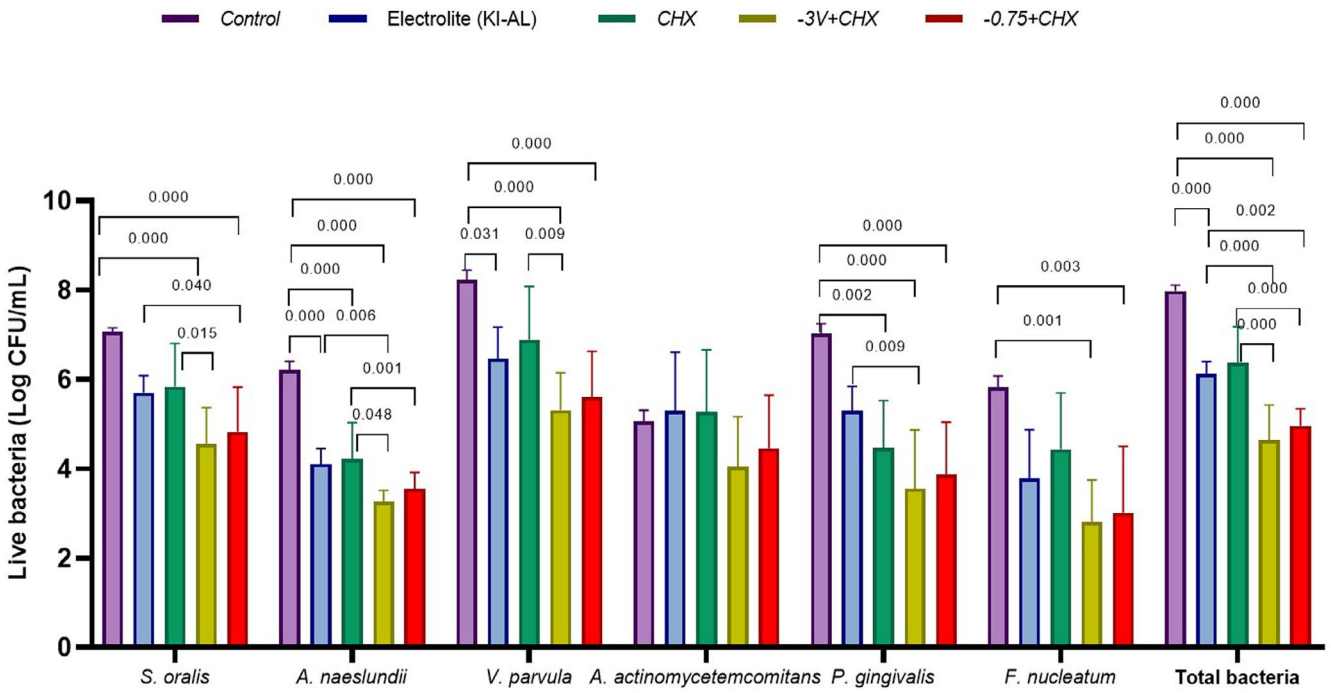

FIGURE 3 | Effects, per treatment groups on the number of viable bacteria in the in vitro multispecies biofilm expressed as colony forming units, CFU mL− [1], obtained by quantitative real-time polymerase chain reaction (qPCR)]. Data are expressed as mean ± standard deviation of the mean (SD). Treatment groups: Control [C], electrolyte [E], 0.12% chlorhexidine [CHX], −3 V and 0.12% CHX [−3 V + CHX], −0.75 V and 0.12% CHX [−0.75 V + CHX].

control − total number of viable bacteria in biofilms treated with electricity)/total number of bacteria in biofilms treated with negative control x100%], the decrease in total bacterial vitality was 52% for the [CHX] group, compared to 99.9% and 99.8% for [−3 V + CHX] and [−0.75 V + CHX] groups, respectively.

5.3 | Effect on Biofilm Structure

Representative SEM images were obtained at three zones of the implant surface (valley, threads and machined neck), before [C] and after the different surface decontamination protocols (Figure 4). In the untreated control group [C], a bacterial cell biomass covered the implant surfaces, with the typical structure of a mature multispecies characterized by clusters of spindle-shaped rods and streptococcal chains, corresponding to *F. nucleatum* and *S. oralis*, respectively. Biofilm bacteria were evident at the threads, in the area between threads (valleys), as well as in the machined neck. After immersion in the electrolyte (KI-AL) [E] or 0.12% CHX [CHX], a dense bacterial biomass was still present, being more pronounced on the moderately rough surfaces, compared to the machined surface at the machined neck. In implants subjected to electrochemical decontamination, [−3 V + CHX] and [−0.75 V + CHX], there was a clear reduction in the bacterial presence with an almost complete biofilm removal, making the implant surface clearly visible, with only scattered cocci and elongated bacteria on the implant surface, together with cell debris and mucopolysaccharide remnants. Moreover, both combined treatments were similarly effective in the three studied areas (threads, valleys, machined necks).

5.4 | Effect on Bacterial Biomass

Figure 5 depicts the area of residual bacteria in each implant zone in the different control and test implants. The mean biofilm area in the untreated group [C] was 334.4 ± 6.9 μm^2 at threads, 319.2 ± 24.6 μm^2 in valleys, and 361.1 ± 6.53 μm^2 in machined necks. In the groups of [E] and [CHX], the area of residual bacteria was higher on the threads and valleys (moderately rough surfaces) on the implant surface, compared to the machined neck (machined surface). In the electrolyte group [E], the mean area of residual bacteria at the thread was 302.2 ± 13.8 μm^2 (90%, $p < 0.001$), at the valley, 221.1 ± 3.5 μm^2 (69%, $p = 0.004$) and at the machined neck, 121.7 ± 4.5 μm^2 (33%). Similar results were obtained for [CHX], where the mean areas of residual bacteria were 245.3 ± 5.7 μm^2 (73%, $p = 0.003$), 259.9 ± 15.6 μm^2 (81%, $p = 0.002$) and 104.5 ± 8.5 μm^2 (29%), at thread, valley, and machined neck, respectively. In both groups combining electrolytic and chemical disinfection, a significant level of decontamination was observed, irrespective of the implant zone, resulting in mean areas of residual bacteria of 0.6 ± 0.3 μm^2 (thread), 0.4 ± 0.1 μm^2 (valley) and 0.5 ± 0.1 μm^2 (machined neck) in the [−3 V + CHX] group and of 5.6 ± 7.1 μm^2 (thread), 3.0 ± 3.2 μm^2 (valley) and 18.8 ± 1.0 μm^2 (machined neck) in the [−0.75 V + CHX] group. Both protocols were able to significantly reduce biofilms when compared to the control group [C] ($p < 0.001$), electrolyte [E] ($p < 0.001$) and [CHX] ($p < 0.001$), but there were no statistically significant differences between both combined treatment groups in any of the studied areas. The biofilm remaining was almost 0 on each of the surfaces evaluated in the [−3 V + CHX] group and 0.9%, 1.7%, and 5% in the threads, valleys, and machined necks, respectively, in the [−0.75 V + CHX] group.

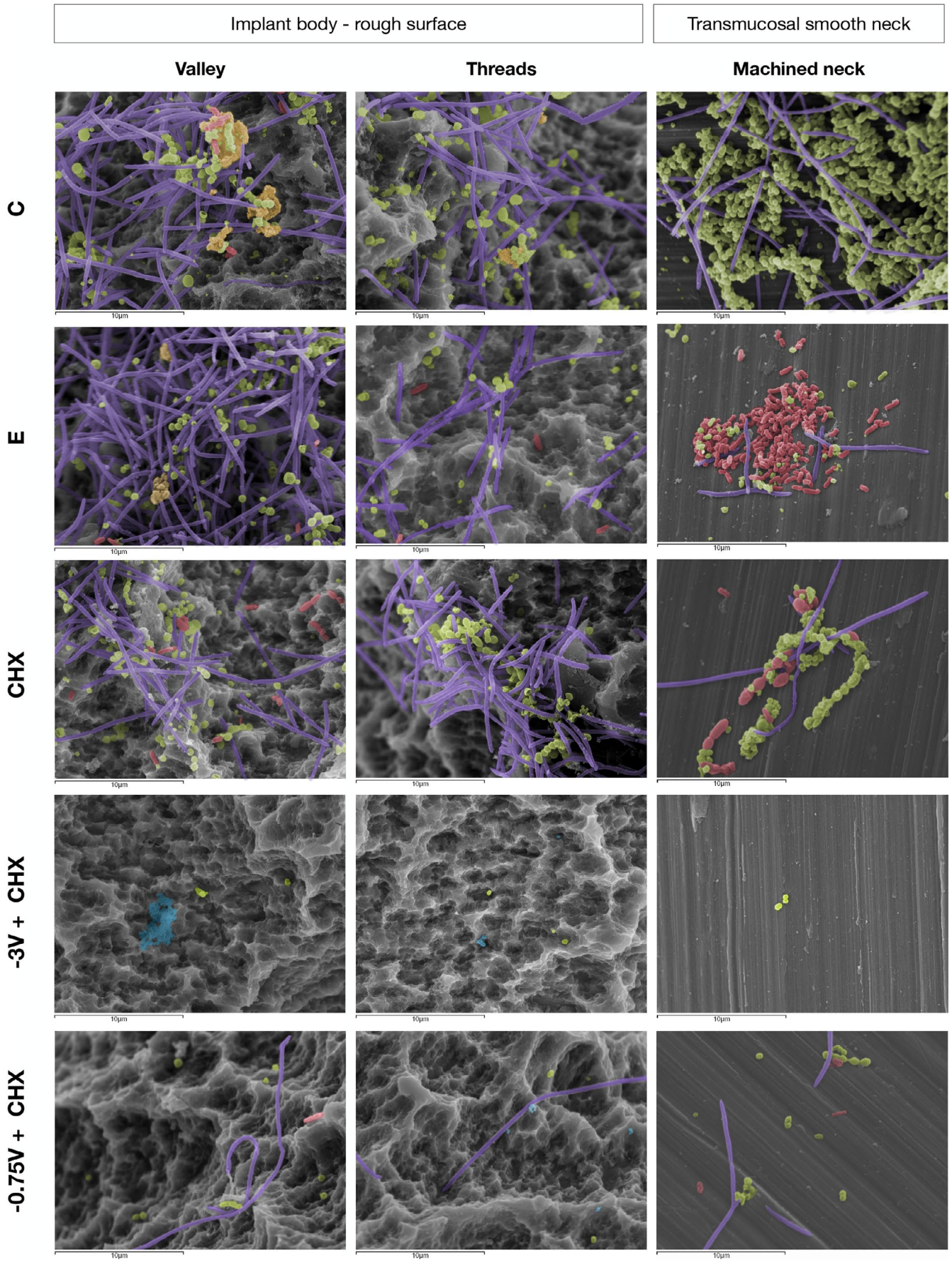

FIGURE 4 | Legend on next page.

FIGURE 4 | Scanning electron microscopy (SEM) of 72-h biofilms after the different treatments applied. It can be observed the different bacterial disposition as well as the different three-dimensional structure of the biofilms in threads, valleys and transmucosal machined necks. Spherical-shaped (green), rod-shaped (red) and spindle-shaped (purple) bacteria were detected, as well as some mucopolysaccharide (yellow) and cell debris (blue). Magnification: 5000×. Scale bar = 10 μm. Treatment groups: Control [C], electrolyte [E], 0.12% chlorhexidine [CHX], −3 V and 0.12% CHX [−3 V + CHX], −0.75 V and 0.12% CHX [−0.75 V + CHX].

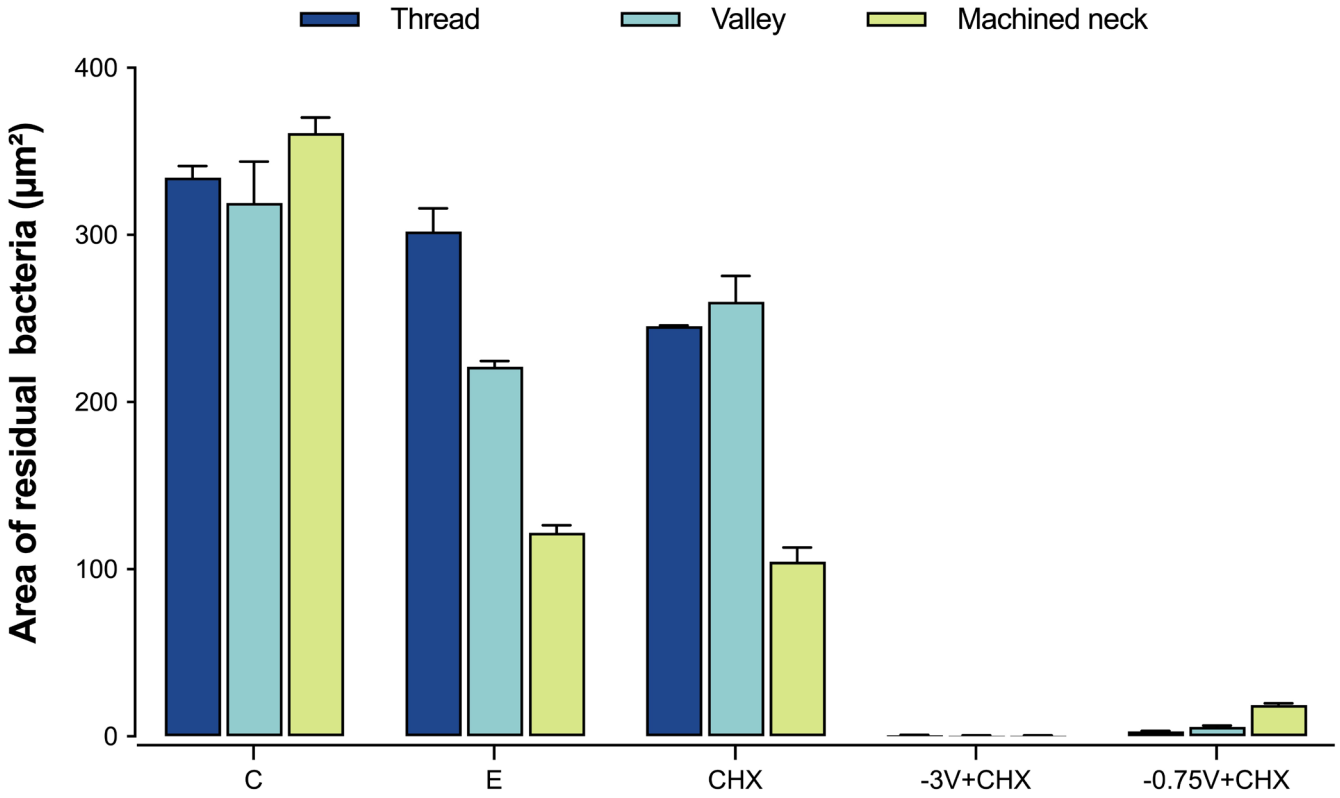

FIGURE 5 | Area of residual bacteria (μm²) on each implant zone (thread, valley, machined) by groups: Control [C], electrolyte [E], 0.12% chlorhexidine [CHX], −3 V and 0.12% CHX [−3 V + CHX], −0.75 V and 0.12% CHX [−0.75 V + CHX].

6 | Discussion

Results from the present in vitro investigation provided clear evidence for the working hypothesis that low-voltage pulses significantly enhanced the antimicrobial effect of chlorhexidine. Potentials as low as −0.75 V demonstrated improvement in the antimicrobial efficacy of 0.12% CHX and also significantly affected the vitality and structure of the multispecies biofilm formed on the titanium implant surfaces, as evidenced by qPCR and SEM. This effect on the number of bacteria and on the biofilm structure was not enhanced when the potential was increased to −3 V.

In a previous report (Virto et al. 2023), our research group demonstrated the ability of an innovative electrochemical treatment using low-intensity electrical currents (a constant-voltage pulse of −3 V during a short exposure of 5 min) to affect the structure and vitality of a 72-h mature subgingival oral biofilm, being able to reduce the total bacterial load in > 99%, while low-voltage pulses had minimal antibacterial effects, with only 2.2% in bacterial biomass reduction, with minimal impact on the tested bacterial species and even showing a minor proliferation in some of them (Virto et al. 2023). Similarly, in the present study, the application of 0.12% CHX alone did not exert a substantial antibacterial effect, with a decrease in total bacterial vitality of 52%, and only a significant impact on *A. naeslundi* and *P. gingivalis*. However, when combining the electrochemical treatment with 0.12% CHX, there was a clear synergistic effect, with bacterial vitality reduced to nearly undetectable levels in both conditions, for the groups [−3 V + CHX] and [−0.75 V + CHX], respectively.

The combined treatment at low voltage [−0.75 V + CHX] group resulted in antibacterial effects comparable to those observed with the −3 V [−3 V + CHX] group, indicating that increasing the potential did not enhance antibacterial efficacy. Some studies have proposed that there may be an intensity threshold above which the bioelectric effect ceases and becomes bactericidal (Costerton et al. 1994). Our findings suggest that this threshold may lie between −0.75 V and −3 V, as high-voltage pulses alone showed substantial antibacterial effects (99.1% reduction) (Virto et al. 2023), but its combination with 0.12% CHX did not significantly increase this effect (99.9% reduction). In contrast, the use of very low potential (−0.75 V) combined with an antiseptic compound (0.12% CHX) showed a clear synergistic

effect. This synergistic effect between the electrochemical treatment and the increase in efficacy of antimicrobial compounds has been previously demonstrated (Blenkinsopp et al. 1992; Costerton et al. 1994; Jass et al. 1995; Mohn et al. 2011; Niepa et al. 2016; Nodzo et al. 2015; Stewart et al. 1999; Sultana et al. 2015; Suttasattakrit et al. 2021; Zou et al. 2022), with a significant decrease (from 1.5 to 4.0 times) in the minimum inhibitory concentration of different antibiotics, such as tobramycin (Costerton et al. 1994; Jass et al. 1995), vancomycin (Nodzo et al. 2015), metronidazole, and amoxicillin (Zou et al. 2022). However, only two in vitro studies testing mono-species biofilms of *P. gingivalis* (Lasserre et al. 2015) and *Escherichia coli* (Kaiser et al. 2020) have evaluated the combined effect of direct currents with commonly used oral antiseptics, such as CHX. In the first of these investigations, the use of low (1.5 mA) and high (10 mA) current intensities during 10 min, followed by 0.2% CHX, was evaluated. Only high current intensities of 10 mA were able to significantly improve the efficacy of 0.2% CHX by reducing *P. gingivalis* biofilms (98.9%), compared to 0.2% CHX alone (87.3%). However, with the use of lower intensities (1.5 mA), there was not a synergistic effect (79.1% vs. 81.1%, respectively) (Lasserre et al. 2015). These results are in contrast with those from the present study where a significant bioelectric effect was demonstrated when applying low potentials (−0.75 V) during a brief 5 min exposure in combination with a lower concentration of CHX (0.12%), this effect being similar to using the same combination but with higher intensity pulses at −3 V. This can be explained by the use of different surfaces where the biofilms were formed. While in the study by (Lasserre et al. 2015), hydroxyapatite disks were placed between the two electrodes responsible for the polarization, in the present study, the biofilm was formed on the stimulation electrode (dental implant), where the electrochemical phenomena occurs, which clearly increases the bioelectric effect. The second study evaluated low current densities (ranging from 0.25 to 2 mA/cm^2) over 9 min, with and without varying CHX concentrations (0.001%, 0.01% and 0.1%), for treating *E. coli* biofilms formed over titanium disks. The authors showed that when the proposed treatments were used alone, they were ineffective (0.25 mA/cm^2 and 0.001% CHX), but when combined they achieved significantly higher cell death rates, with 91% dead cells compared to 44% and 36%, respectively (Kaiser et al. 2020). Another differential factor between these studies and the present investigation is that while the two cited studies (Kaiser et al. 2020; Lasserre et al. 2015) used single-species biofilms, the present investigation used a validated multispecies oral biofilm containing six representative bacterial species formed on real titanium dental implants.

The mechanisms of action underneath the enhancement of antimicrobial efficacy by low-intensity electric currents require further investigation. Some authors have suggested that low-voltage electrical currents may disrupt biofilm matrix charges, allowing antimicrobial agents to diffuse inside the biofilm and reach the target cells (Freebairn et al. 2013) or alter the electrical potential of the cell membrane, opening pores and thus facilitating the penetration of antimicrobials into deeper layers (Cevc 1990; Costerton et al. 1994). Other theories suggest that electrical currents may increase the metabolic activity of biofilm cells by producing more dissolved oxygen, which is crucial for their growth, making them more susceptible to antimicrobials (Stewart et al. 1999), or even upregulate genes related to antibiotic resistance and small molecule transport such as porin gene expression (Niepa et al. 2016; Zou et al. 2022).

One additional positive effect demonstrated in this study by combining the electrochemical with the antiseptic effect is its uniform antibiofilm effect independent from the implant macro and microtopography (threads, valleys or the machined polished neck), while it is well established that implant topography and surface characteristics have a significant impact not only on how biofilms form but also on the effectiveness of the different tested decontamination methods used in the treatment of peri-implantitis (Albouy et al. 2011; Ichioka et al. 2023; Sanz-Martín et al. 2021; Steiger-Ronay et al. 2017). Different studies have shown that in implants with high thread pitch, such as the Straumann tissue-level implants used in this investigation, the machined surface area is the easiest to decontaminate, followed by the thread tips, with the apically facing threads and the valleys being the most difficult areas to reach with conventional mechanical instruments (e.g., curettes, ultrasonic devices, air-powder abrasive devices and titanium brushes) (Ichioka et al. 2023; Sanz-Martín et al. 2021; Steiger-Ronay et al. 2017). Electrochemical decontamination, however, has shown a uniform efficacy, likely because the electric current can reach all areas, even within the implant surface itself. Thus, while additional studies are needed to better understand the intrinsic mechanisms of action in electrochemical disinfection, it is clear that with this method surface topography may not be such a critical factor for effective decontamination.

From an electrical standpoint, these results are particularly relevant since the use of low and very low intensity currents results in a significant reduction in energy consumption, while maintaining a significant antibacterial effect. The use of the combined protocol resulted in a 99.98% decrease in energy consumption, a notable benefit given the current increasing emphasis on environmental sustainability. Another important advantage of using low intensity currents is the increase in patients safety by minimizing its morbidity on intraoral applications. Although studies on the cytotoxicity of electrochemical decontamination are limited, existing histological findings indicate that exposure to high electrical currents (32–400 mA) causes significant epithelial and connective tissue damage (Al-Hashedi et al. 2016). Indeed, soft tissue dehiscence has been observed within the first weeks following electrolytic cleaning and regenerative therapy of peri-implantitis (Bosshardt et al. 2022; Schlee et al. 2021). Moreover, a recently published study has also demonstrated, in an in vitro peri-implant mucosal model, that electrolytic cleaning with Galvosurge (600 mA) showed clear cytotoxic effects with disruption of tissue layers and cell vitality reduction of 85% (Alonso-Español et al. 2025). In contrast, our group has demonstrated that the low-intensity electrical currents used in the present study have no detrimental effect on the viability of pre-osteoblast cells (Cai et al. 2024) and, thus, the proposed treatment may offer a safer, more patient-friendly approach to electrolytic cleaning, reducing the need for anesthesia or its application only with surgical interventions. However, different studies have reported altered cytocompatibility after CHX application, showing a clear impact on the mucosal integrity, alteration of cell vitality, and decrease in cell adhesion (Alonso-Español et al. 2025). Given that the present study was designed for proof-of-concept purposes, we selected CHX as it is the gold

standard. Future studies should evaluate the cytotoxicity of the proposed combined treatments, as well as the combination with low-dose CHX and other antimicrobials.

Nevertheless, the results of the present investigation should be interpreted with caution due to the in vitro nature of the experimental model and the use of a static biofilm model since these conditions do not fully replicate the complex nutrients, physicochemical (e.g., pH and redox potential), and flow conditions of the oral cavity and/or the subgingival/submarginal environments. In addition, while the present study provides proof-of-concept data, the limited sample size may contribute to the observed variability in the qPCR results. Future studies should consider increasing the number of biological replicates. Based on the current effect size (~1.7-log reduction) and standard deviation, an estimated 12 samples per group would be necessary to detect statistically significant differences with 80% power at a 5% significance level. Further in vivo studies are also needed to confirm these findings. Additionally, both electrodes were immersed in a single electrolyte within the electrochemical cell, which does not rule out that reactions at the counter electrode might exert antibacterial effects on the implant surface through the diffusion of reactive products. Alternative designs using agar or conductive membranes to separate the electrodes (Mohn et al. 2011; Schneider et al. 2018) could allow electrical conduction while isolating chemical reactions, although such designs may increase resistance and, consequently, increase energy consumption.

Future studies should initially aim to elucidate the underlying mechanisms of biofilm disruption by assessing potential changes in membrane integrity, metabolic activity, and reactive oxygen species (ROS) generation in treated biofilms. In parallel, transcriptomic analyses should be performed to identify differentially expressed genes related to stress responses and membrane-associated functions, such as porin gene expression. Following these mechanistic insights, cytotoxicity assays should be conducted to evaluate the safety of the low-voltage + CHX treatment on host tissues. Ultimately, in vivo validation will be carried out using relevant animal models to assess the efficacy and biocompatibility of the proposed therapy under clinically relevant conditions. Another important issue that remains to be elucidated is whether the proposed treatment is effective in reducing or eliminating hard calculus deposits. Indeed, some authors have suggested that chemical or electrical decontamination alone may not be sufficient for removing these hard deposits, so they should be combined with mechanical instrumentation. Future research should evaluate the efficacy of low-voltage electrical currents with CHX for calculus removal.

In conclusion, despite these limitations, the results suggest that low-intensity direct currents may significantly enhance the efficacy of a widely used oral antiseptic, such as chlorhexidine digluconate. The tested protocol effectively reduced the vitality of mature multispecies biofilms and minimized residual bacteria on authentic dental implant surfaces, achieving > 95% biofilm removal with voltages as low as −0.75 V, irrespective of the implant zone. This approach offers promising potential for the treatment of peri-implant diseases.

Author Contributions

Verónica Odeh: writing – original draft, formal analysis, conceptualization, investigation, methodology. **Leire Virto:** formal analysis, conceptualization, writing – review and editing, data curation. **Enrique Garcia-Quismondo:** formal analysis, writing – review and editing, conceptualization. **David Herrera:** writing – review and editing, supervision, conceptualization. **Jesús Palma:** supervision, writing – review and editing, conceptualization. **Mariano Sanz:** writing – review and editing, supervision, conceptualization.

Acknowledgments

The authors are grateful to Ana Vicente, Myriam González, and ICTS National Centre of Electronic Microscopy (International Excellence Campus of Moncloa, University Complutense of Madrid, Spain) for their invaluable support in microscopy techniques.

Conflicts of Interest

The authors have stated explicitly that there are no conflicts of interest in connection with this work.

Data Availability Statement

The data that support the findings of this study are available from the corresponding author upon reasonable request.

References

Albouy, J. P., I. Abrahamsson, L. G. Persson, and T. Berglundh. 2011. "Implant Surface Characteristics Influence the Outcome of Treatment of Peri-Implantitis: An Experimental Study in Dogs." *Journal of Clinical Periodontology* 38, no. 1: 58–64. https://doi.org/10.1111/j.1600-051X.2010.01631.x.

Al-Hashedi, A. A., M. Laurenti, M.-N. Abdallah, R. F. Albuquerque Jr., and F. Tamimi. 2016. "Electrochemical Treatment of Contaminated Titanium Surfaces In Vitro: An Approach for Implant Surface Decontamination." *ACS Biomaterials Science & Engineering* 2, no. 9: 1504–1518. https://doi.org/10.1021/acsbiomaterials.6b00265.

Alonso-Español, A., E. Bravo, A. Carrillo de Albornoz, et al. 2025. "Antimicrobial Effect and Cytocompatibility After Using Different Decontamination Methods on Titanium Implant Surfaces: An in Vitro Study." *Clinical Oral Implants Research* 36, no. 5: 626–639. https://doi.org/10.1111/clr.14410.

Bermejo, P., M. C. Sánchez, A. Llama-Palacios, E. Figuero, D. Herrera, and M. Sanz. 2019. "Topographic Characterization of Multispecies Biofilms Growing on Dental Implant Surfaces: An in Vitro Model." *Clinical Oral Implants Research* 30, no. 3: 229–241. https://doi.org/10.1111/clr.13409.

Blenkinsopp, S. A., A. E. Khoury, and J. W. Costerton. 1992. "Electrical Enhancement of Biocide Efficacy Against *Pseudomonas aeruginosa* Biofilms." *Applied and Environmental Microbiology* 58, no. 11: 3770–3773. https://doi.org/10.1128/aem.58.11.3770-3773.1992.

Bosshardt, D. D., U. R. Brodbeck, F. Rathe, et al. 2022. "Evidence of Re-Osseointegration After Electrolytic Cleaning and Regenerative Therapy of Peri-Implantitis in Humans: A Case Report With Four Implants." *Clinical Oral Investigations* 26, no. 4: 3735–3746. https://doi.org/10.1007/s00784-021-04345-1.

Cai, W., M. Wang, A. E. Hadad, et al. 2024. "The Effect of Titanium Surface Treatment by Application of Constant Potential or Current on the Viability of Pre-Osteoblast Cells: An In-Vitro Study." *Frontiers in Bioengineering and Biotechnology* 12: 1425450. https://doi.org/10.3389/fbioe.2024.1425450.

Canty, M., N. Luke-Marshall, A. Campagnari, and M. Ehrensberger. 2017. "Cathodic Voltage-Controlled Electrical Stimulation of Titanium for Prevention of Methicillin-Resistant Staphylococcus Aureus and *Acinetobacter baumannii* Biofilm Infections." *Acta Biomaterialia* 48: 451–460. https://doi.org/10.1016/j.actbio.2016.11.056.

Cevc, G. 1990. "Membrane electrostatics." *Biochimica et Biophysica Acta* 1031, no. 3: 311–382. https://doi.org/10.1016/0304-4157(90)90015-5.

Cosgarea, R., A. Roccuzzo, K. Jepsen, A. Sculean, S. Jepsen, and G. E. Salvi. 2023. "Efficacy of Mechanical/Physical Approaches for Implant Surface Decontamination in Non-Surgical Submarginal Instrumentation of Peri-Implantitis. A Systematic Review." *Journal of Clinical Periodontology* 50, no. Suppl 26: 188–211. https://doi.org/10.1111/jcpe.13762.

Costerton, J. W., B. Ellis, K. Lam, F. Johnson, and A. E. Khoury. 1994. "Mechanism of Electrical Enhancement of Efficacy of Antibiotics in Killing Biofilm Bacteria." *Antimicrobial Agents and Chemotherapy* 38, no. 12: 2803–2809. https://doi.org/10.1128/aac.38.12.2803.

de Waal, Y. C. M., L. Winning, A. Stavropoulos, and I. Polyzois. 2023. "Efficacy of Chemical Approaches for Implant Surface Decontamination in Conjunction With Sub-Marginal Instrumentation, in the Non-Surgical Treatment of Peri-Implantitis: A Systematic Review." *Journal of Clinical Periodontology* 50, no. Suppl 26: 212–223. https://doi.org/10.1111/jcpe.13749.

Del Pozo, J. L., M. S. Rouse, and R. Patel. 2008. "Bioelectric Effect and Bacterial Biofilms. A Systematic Review." *International Journal of Artificial Organs* 31, no. 9: 786–795. https://doi.org/10.1177/039139880803100906.

Ehrensberger, M. T., M. E. Tobias, S. R. Nodzo, et al. 2015. "Cathodic Voltage-Controlled Electrical Stimulation of Titanium Implants as Treatment for Methicillin-Resistant *Staphylococcus Aureus* Periprosthetic Infections." *Biomaterials* 41: 97–105. https://doi.org/10.1016/j.biomaterials.2014.11.013.

Freebairn, D., D. Linton, E. Harkin-Jones, D. S. Jones, B. F. Gilmore, and S. P. Gorman. 2013. "Electrical Methods of Controlling Bacterial Adhesion and Biofilm on Device Surfaces." *Expert Review of Medical Devices* 10, no. 1: 85–103. https://doi.org/10.1586/erd.12.70.

Ichioka, Y., L. Virto, P. Nuevo, et al. 2023. "Decontamination of Biofilm-Contaminated Implant Surfaces: An in Vitro Evaluation." *Clinical Oral Implants Research* 34, no. 10: 1058–1072. https://doi.org/10.1111/clr.14136.

Jass, J., J. W. Costerton, and H. M. Lappin-Scott. 1995. "The Effect of Electrical Currents and Tobramycin on *Pseudomonas aeruginosa* Biofilms." *Journal of Industrial Microbiology* 15, no. 3: 234–242. https://doi.org/10.1007/bf01569830.

Jass, J., and H. M. Lappin-Scott. 1996. "The Efficacy of Antibiotics Enhanced by Electrical Currents Against *Pseudomonas aeruginosa* Biofilms." *Journal of Antimicrobial Chemotherapy* 38, no. 6: 987–1000. https://doi.org/10.1093/jac/38.6.987.

Kaiser, F., D. Scharnweber, S. Bierbaum, and C. Wolf-Brandstetter. 2020. "Success and Side Effects of Different Treatment Options in the Low Current Attack of Bacterial Biofilms on Titanium Implants." *Bioelectrochemistry* 133: 107485. https://doi.org/10.1016/j.bioelechem.2020.107485.

Koch, M., M. Göltz, M. Xiangjun, M. Karl, S. Rosiwal, and A. Burkovski. 2020. "Electrochemical Disinfection of Dental Implants Experimentally Contaminated With Microorganisms as a Model for Periimplantitis." *Journal of Clinical Medicine* 9, no. 2: 475. https://doi.org/10.3390/jcm9020475.

Lasserre, J. F., J. G. Leprince, S. Toma, and M. C. Brecx. 2015. "Electrical Enhancement of Chlorhexidine Efficacy Against the Periodontal Pathogen *Porphyromonas Gingivalis* Within a Biofilm." *New Microbiology* 38, no. 4: 511–519.

Marin, M. J., N. Ambrosio, D. Herrera, M. Sanz, and E. Figuero. 2018. "Validation of a Multiplex qPCR Assay for the Identification and Quantification of Aggregatibacter Actinomycetemcomitans and *Porphyromonas gingivalis*: In Vitro and Subgingival Plaque Samples." *Archives of Oral Biology* 88: 47–53. https://doi.org/10.1016/j.archoralbio.2018.01.012.

Marin, M. J., E. Figuero, D. Herrera, and M. Sanz. 2017. "Quantitative Analysis of Periodontal Pathogens Using Real-Time Polymerase Chain Reaction (PCR)." *Methods in Molecular Biology* 1537: 191–202. https://doi.org/10.1007/978-1-4939-6685-1_11.

Mohn, D., M. Zehnder, W. J. Stark, and T. Imfeld. 2011. "Electrochemical Disinfection of Dental Implants-a Proof of Concept." *PLoS One* 6, no. 1: e16157. https://doi.org/10.1371/journal.pone.0016157.

Niepa, T. H., L. M. Snepenger, H. Wang, et al. 2016. "Sensitizing *Pseudomonas Aeruginosa* to Antibiotics by Electrochemical Disruption of Membrane Functions." *Biomaterials* 74: 267–279. https://doi.org/10.1016/j.biomaterials.2015.10.007.

Nodzo, S., M. Tobias, L. Hansen, et al. 2015. "Cathodic Electrical Stimulation Combined With Vancomycin Enhances Treatment of Methicillin-Resistant *Staphylococcus Aureus* Implant-Associated Infections." *Clinical Orthopaedics and Related Research* 473, no. 9: 2856–2864. https://doi.org/10.1007/s11999-015-4280-3.

Ramanauskaite, A., F. Schwarz, E. A. Cafferata, and P. Sahrmann. 2023. "Photo/Mechanical and Physical Implant Surface Decontamination Approaches in Conjunction With Surgical Peri-Implantitis Treatment: A Systematic Review." *Journal of Clinical Periodontology* 50, no. Suppl 26: 317–335. https://doi.org/10.1111/jcpe.13783.

Sahrmann, P., M. Zehnder, D. Mohn, A. Meier, T. Imfeld, and T. Thurnheer. 2014. "Effect of Low Direct Current on Anaerobic Multispecies Biofilm Adhering to a Titanium Implant Surface." *Clinical Implant Dentistry and Related Research* 16, no. 4: 552–556. https://doi.org/10.1111/cid.12018.

Sanchez, M. C., A. Llama-Palacios, E. Fernandez, et al. 2014. "An in Vitro Biofilm Model Associated to Dental Implants: Structural and Quantitative Analysis of in Vitro Biofilm Formation on Different Dental Implant Surfaces." *Dental Materials* 30, no. 10: 1161–1171. https://doi.org/10.1016/j.dental.2014.07.008.

Sánchez, M. C., M. J. Marín, E. Figuero, et al. 2014. "Quantitative Real-Time PCR Combined With Propidium Monoazide for the Selective Quantification of Viable Periodontal Pathogens in an in Vitro Subgingival Biofilm Model." *Journal of Periodontal Research* 49, no. 1: 20–28. https://doi.org/10.1111/jre.12073.

Sanz-Martín, I., K. Paeng, H. Park, J. K. Cha, U. W. Jung, and M. Sanz. 2021. "Significance of Implant Design on the Efficacy of Different Peri-Implantitis Decontamination Protocols." *Clinical Oral Investigations* 25, no. 6: 3589–3597. https://doi.org/10.1007/s00784-020-03681-y.

Schlee, M., H. L. Wang, T. Stumpf, U. Brodbeck, D. Bosshardt, and F. Rathe. 2021. "Treatment of Periimplantitis With Electrolytic Cleaning Versus Mechanical and Electrolytic Cleaning: 18-Month Results From a Randomized Controlled Clinical Trial." *Journal of Clinical Medicine* 10, no. 16: 3475. https://doi.org/10.3390/jcm10163475.

Schneider, S., M. Rudolph, V. Bause, and A. Terfort. 2018. "Electrochemical Removal of Biofilms From Titanium Dental Implant Surfaces." *Bioelectrochemistry* 121: 84–94. https://doi.org/10.1016/j.bioelechem.2018.01.008.

Schwarz, F., J. Derks, A. Monje, and H. L. Wang. 2018. "Peri-implantitis." *Journal of Clinical Periodontology* 45, no. Suppl 20: S246–S266. https://doi.org/10.1111/jcpe.12954.

Solderer, A., M. Kaufmann, D. Hofer, D. Wiedemeier, T. Attin, and P. R. Schmidlin. 2019. "Efficacy of Chlorhexidine Rinses After Periodontal or Implant Surgery: A Systematic Review." *Clinical Oral Investigations* 23, no. 1: 21–32. https://doi.org/10.1007/s00784-018-2761-y.

Steiger-Ronay, V., A. Merlini, D. B. Wiedemeier, P. R. Schmidlin, T. Attin, and P. Sahrmann. 2017. "Location of Unaccessible Implant Surface Areas During Debridement in Simulated Peri-Implantitis Therapy." *BMC Oral Health* 17, no. 1: 137. https://doi.org/10.1186/s12903-017-0428-8.

Stewart, P. S., W. Wattanakaroon, L. Goodrum, S. M. Fortun, and B. R. McLeod. 1999. "Electrolytic Generation of Oxygen Partially Explains Electrical Enhancement of Tobramycin Efficacy Against *Pseudomonas aeruginosa* Biofilm." *Antimicrobial Agents and Chemotherapy* 43, no. 2: 292–296. https://doi.org/10.1128/aac.43.2.292.

Sultana, S. T., J. T. Babauta, and H. Beyenal. 2015. "Electrochemical Biofilm Control: A Review." *Biofouling* 31, no. 9–10: 745–758. https://doi.org/10.1080/08927014.2015.1105222.

Suttasattakrit, K., A. Khamkeaw, C. Tangwongsan, P. Pavasant, and M. Phisalaphong. 2021. "Ionic Silver and Electrical Treatment for Susceptibility and Disinfection of *Escherichia Coli* Biofilm-Contaminated Titanium Surface." *Molecules* 27, no. 1: 180. https://doi.org/10.3390/molecules27010180.

Virto, L., V. Odeh, E. Garcia-Quismondo, et al. 2023. "Electrochemical Decontamination of Titanium Dental Implants. An in Vitro Biofilm Model Study." *Clinical Oral Implants Research* 34, no. 5: 486–497. https://doi.org/10.1111/clr.14055.

Vyas, N., R. L. Sammons, O. Addison, H. Dehghani, and A. D. Walmsley. 2016. "A Quantitative Method to Measure Biofilm Removal Efficiency From Complex Biomaterial Surfaces Using SEM and Image Analysis." *Scientific Reports* 6, no. 1: 32694. https://doi.org/10.1038/srep32694.

Wilensky, A., L. Shapira, A. Limones, and C. Martin. 2023. "The Efficacy of Implant Surface Decontamination Using Chemicals During Surgical Treatment of Peri-Implantitis: A Systematic Review and Meta-Analysis." *Journal of Clinical Periodontology* 50, no. Suppl 26: 336–358. https://doi.org/10.1111/jcpe.13794.

Zou, P., P. Li, J. Liu, P. Cao, and Q. Luan. 2022. "Direct Current Exerts Electricidal and Bioelectric Effects on *Porphyromonas gingivalis* Biofilms Partially via Promoting Oxidative Stress and Antibiotic Transport." *Journal of Microbiology* 60, no. 1: 70–78. https://doi.org/10.1007/s12275-022-1238-5.

Supporting Information

Additional supporting information can be found online in the Supporting Information section. **Table S1.** Effect, per treatment groups, on the number of viable bacteria in the in vitro multispecies biofilm expressed as colony forming units, CFU $mL-^{1}$, obtained by quantitative real-time polymerase chain reaction (qPCR). Data are expressed as mean ± standard deviation of the mean (SD). Treatment groups: control [C], electrolyte [E], 0.12% chlorhexidine [CHX], −3 V and 0.12% CHX [−3 V + CHX], −0.75 V and 0.12% CHX [−0.75 V + CHX].